International Journal of Science and Technology (IJST)
ISSN: 3049-1118, Volume- 3, Issue- 2 (April - June 2026)

Polynomial Approximation Analysis of Transient Mixed Convection Flow in A Vertical Micro-Annulus with Viscous Dissipation

Kufre A. Mkpedem[1*], Mary O. Durojaye[2]
[1]Sheffield Hallam University, United Kingdom.
[2]University of Abuja, Nigeria.

Abstract

This paper presents an analytical assessment of transient mixed convection flow and heat transfer in a vertical micro-annulus, taking into account internal heat generation, viscous dissipation, and temperature-dependent viscosity. The Boussinesq approximation is used to develop the governing momentum and energy equations, which are then translated into dimensionless form. A polynomial approximation method is used to generate closed-form solutions, which are then evaluated via symbolic computation. The effect of critical dimensionless factors, such as the Reynolds number, Peclet number, Eckert number, and heat generation coefficients, on fluid velocity and temperature distributions is investigated. The findings show that internal heat generation greatly increases fluid temperature while decreasing flow velocity. Increasing Eckert and Peclet numbers reduces temperature profiles, while increasing Reynolds numbers decreases fluid velocity. The research also reveals a linked interaction between heat and flow fields, which is controlled by viscosity variations and energy dissipation effects. The findings have important implications for thermal management and flow control in micro-scale systems including microchannels, heat exchangers, and cooling devices, where accurate prediction of linked heat and fluid flow is critical.

Keywords: Annulus, convective flow, heat generation, transient, viscosity.

1. Introduction

Mixed convection flow in micro-scale geometrics geometries has attracted a lot of attention due to its numerous uses in modern engineering systems, such as micro-electro-mechanical systems (MEMS), micro heat exchangers, electronic cooling devices, and biomedical technologies. In these systems, the interaction of induced and natural convection has a substantial impact on thermal performance and flow behaviour. Annular geometries are particularly common in engineering applications such as double-pipe heat exchangers, nuclear reactor cooling systems, and thermal energy storage devices (Abderrahmane et al., 2022; Bouchraba, 2025).

*Corresponding Author Email: kufremkpedem@gmail.com
Published: 25 April 2026
DOI: https://doi.org/10.70558/IJST.2026.v3.i2.241247

Because of substantial temperature gradients, the assumption of constant fluid characteristics is sometimes insufficient for micro-scale flows. Temperature change affects viscosity, which is vital in determining flow resistance and heat transfer characteristics. Temperature-dependent viscosity influences velocity distribution, boundary layer development, and thermal transport processes, hence it must be included in realistic mathematical models (Nabwey, 2024; Vajjha & Das, 2015).

Several research have looked at mixed convection flow in annular and microchannel systems. Jha and Aina (2018) developed an accurate solution for steady mixed convection flow in a vertical micro-annulus with temperature-dependent viscosity, demonstrating that viscosity fluctuation has a major impact on flow behaviour. Similarly, Sheikholeslami and colleagues (2016-2023) conducted substantial research on convection heat transfer in circular geometries, emphasizing the effects of thermal factors and boundary conditions on flow structure and heat transfer rates. More recent studies have included additional effects such as viscous dissipation, entropy generation, and internal heat sources, demonstrating that these factors have a significant impact on thermal performance in constrained geometries (Nabwey, 2024; Bouchraba, 2025).

Despite these contributions, most extant research focus on steady-state circumstances, whereas many practical systems operate in turbulent regimes. Furthermore, few analytical works investigate transient effects, internal heat generation, viscous dissipation, and temperature-dependent viscosity in vertical micro-annular topologies. Addressing these restrictions is critical for improving predictive modelling and the design of micro-scale thermal systems (Jha and Aina, 2018; Sheikholeslami, 2020; Nabwey, 2024).

With the increasing complexity of micro-scale systems, attention has shifted toward analytical methods capable of capturing coupled thermo-fluid behaviour with reduced computational cost. Among these, the polynomial approximation method (PAM) has emerged as an effective semi-analytical technique for solving nonlinear governing equations in convection problems. The method involves assuming polynomial trial functions for velocity and temperature fields, which are substituted into the governing equations to obtain approximate closed-form solutions. This approach provides a balance between analytical tractability and physical accuracy, particularly for transient problems where exact solutions are often difficult to obtain (Finlayson, 1972; Reddy, 1993; Bejan, 2013).

Polynomial approximation methods outperform purely numerical alternatives, such as finite element or meshless methods, in terms of processing efficiency and physical insight. Numerical methods, such as radial basis function-based meshless techniques, have been used successfully to accurately simulate mixed convection problems; however, they frequently require significant computational resources and may not provide explicit relationships between governing parameters and flow variables (Bartwal et al., 2025). PAM, on the other hand, produces explicit expressions that

make parametric analysis easier and improve comprehension of the underlying physical processes.

In this study, an analytical model is created to explore transient mixed convection flow and heat transmission in a vertical micro-annulus. The model considers temperature-dependent viscosity, viscous dissipation, and internal heat generation. The governing equations are stated using the Boussinesq approximation to conserve momentum and energy, and then solved analytically using a polynomial approximation approach. The implications of critical dimensionless parameters on velocity and temperature distributions are investigated to gain a better understanding of the coupled thermo-fluid behaviour in micro-scale annular systems.

2. Model Formulation

Based on Jha and Aina (2018), the fluid inside the annulus is believed to generate or absorb energy. The z-axis runs vertically up the cylinder's axis, and radius is the radial direction. The inner and outer cylinders have radiuses r_1 and r_2, respectively, as indicated in Figure 1 below.

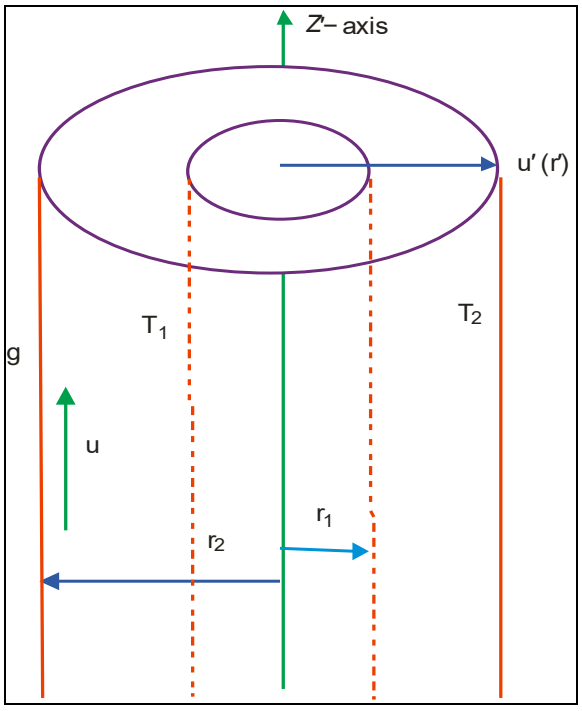

Figure 1: Flow Structure

The viscous dissipation and compressibility effect in the fluid are considered using the Boussinesq approximation, and the mathematical model expressing the current physical state can be described as:

$$\rho_0\left(\frac{\partial u}{\partial t}+v_o\frac{\partial u}{\partial r}\right)=-\frac{\partial p}{\partial z}+\frac{1}{r}\frac{\partial}{\partial r}\left(\mu r\frac{\partial u}{\partial r}\right)+g\beta\rho_0\left(T-T_0\right) \quad (1)$$

$$\rho_0\left(\frac{\partial T}{\partial t}+v_o\frac{\partial T}{\partial r}\right)=\frac{k}{r}\frac{\partial}{\partial r}\left(r\frac{\partial u}{\partial r}\right)+\mu\left(\frac{\partial u}{\partial r}\right)^2+q''' \quad (2)$$

The temperature dependent viscosity is [8]:

$$\mu = \mu_0 \exp\left(-b\left(T - T_0\right)\right) \tag{3}$$

The internal heat generation or depletion term q''' is modeled [9] as:

$$q''' = \frac{\rho_0 c_p U_{s1}^2}{v_0}\left(a^*\left(T_w - T_0\right)e^{-\frac{U_{s1}}{v_0}r} + b^*\left(T - T_0\right)\right) \tag{4}$$

The first term indicates the reliance of internal heat generation or absorption on space coordinates, while the last term represents the dependence on temperature within the boundary layer. When both $a^* > 0$ and $b^* > 0$ heat is generated, whereas when both $a^* < 0$ and $b^* < 0$ heat is depleted.

The initial and boundary conditions are given below:

$$\left.\begin{aligned} &u\left(r,0\right) = 0, \quad u\left(r_1,t\right) = U_{s1}, \quad -K_n D_n \left.\frac{\partial u}{\partial r}\right|_{r=r_2} = 0 \\ &T\left(r,0\right) = T_0, \quad T\left(r_1,t\right) = T_{s1}, \quad -\frac{K_n D_n}{\mathrm{P}\,r}\left.\frac{\partial T}{\partial r}\right|_{r=r_2} = 0 \end{aligned}\right\} \tag{5}$$

Where a^* represent the coefficient of space-dependent internal heat generation or absorption, b^* represent the coefficient of temperature-dependent internal heat generation or absorption, ρ_o represent the mass density of T_o , T_o represent the reference fluid temperature, , ensuring a liner relationship between the local density and the level temperature, The reference temperature is chosen as the mean fluid temperature in any cross section of the micro-annulus μ_o represent the viscosity when temperature is T_o , υ is Kinematic viscosity, t is time, α I sThermal diffusivity, Re is Reynold number, T is the temperature of the fluid, q''' is the internal heat generation or depletion term.

3.0 Method of Solution

3.1: Dimensional Analysis

The following parameters are defined to represent the problem in a non-dimensional way.

$$\begin{aligned} &r' = \frac{r}{r_2}, \quad r^* = \frac{r_1}{r_2}, \quad z' = \frac{z}{\mathrm{Re}\,Dh}, \quad t' = \frac{U_{s1}t}{r_2}, \quad \phi = \frac{u}{U_{s1}}, \quad p' = \frac{p}{\rho_0 U_{s1}^2}, \\ &Dh = 2\left(r_2 - r_1\right), \quad v = \frac{v_0}{U_{s1}}, \quad \theta = \frac{T - T_0}{T_{s1} - T_0} \end{aligned} \tag{6}$$

Using (6), and dropping the prime, equations (1)-(3) becomes

$$\left(\frac{\partial \phi}{\partial t} + v\frac{\partial \phi}{\partial r}\right) = -d\frac{\partial p}{\partial z} + \frac{1}{\mathrm{Re}\,r}\frac{\partial}{\partial r}\left(re^{-c\theta}\frac{\partial \phi}{\partial r}\right) + G_{r\theta}\theta \tag{7}$$

$$\left(\frac{\partial\theta}{\partial t}+v\frac{\partial\theta}{\partial r}\right)=\frac{1}{Per}\frac{\partial}{\partial r}\left(r\frac{\partial\theta}{\partial r}\right)+\frac{Ec}{\mathrm{Re}}e^{-c\theta}\left(\frac{\partial\phi}{\partial r}\right)^2+\mathrm{Re}\left(a^*e^{-\mathrm{Re}r}+b^*\theta\right) \tag{8}$$

$$\left.\begin{aligned}\phi(r,0)=0,\quad \phi\left(r^*,\mathrm{t}\right)=1,\quad \left.\frac{\partial\phi}{\partial r}\right|_{r=1}=0\\ \theta(r,0)=0,\quad \theta\left(r^*,\mathrm{t}\right)=1,\quad \left.\frac{\partial\theta}{\partial r}\right|_{r=1}=0\end{aligned}\right\} \tag{9}$$

Applying coordinate transformation

$$\frac{\partial}{\partial r}\rightarrow\frac{\partial}{\partial\eta}\frac{\partial\eta}{\partial r}=\frac{\partial}{\partial\eta} \tag{10}$$

$$\frac{\partial}{\partial t}\rightarrow\frac{\partial}{\partial\eta}\frac{\partial\eta}{\partial t}+\frac{\partial}{\partial t}=-u\frac{\partial}{\partial\eta}+\frac{\partial}{\partial t} \tag{11}$$

We have

$$\frac{\partial\phi}{\partial t}=-d\frac{\partial p}{\partial z}+\frac{1}{\mathrm{Re}\eta}\frac{\partial}{\partial\eta}\left(\eta(1-c\theta)\frac{\partial\phi}{\partial\eta}\right)+G_{r\theta}\theta \tag{12}$$

$$\frac{\partial\theta}{\partial t}=\frac{1}{Pe\eta}\frac{\partial}{\partial\eta}\left(\eta\frac{\partial\theta}{\partial\eta}\right)+\frac{Ec}{\mathrm{Re}}(1-c\theta)\left(\frac{\partial\phi}{\partial\eta}\right)^2+\mathrm{Re}\left(a^*e^{-\mathrm{Re}r}+b^*\theta\right) \tag{13}$$

$$\left.\begin{aligned}\phi(\eta,0)=0,\quad \phi\left(r^*,\mathrm{t}\right)=1,\quad \left.\frac{\partial\phi}{\partial\eta}\right|_{\eta=1}=0\\ \theta(\eta,0)=0,\quad \theta\left(r^*,\mathrm{t}\right)=1,\quad \left.\frac{\partial\theta}{\partial\eta}\right|_{\eta=1}=0\end{aligned}\right\} \tag{14}$$

Where,

Gr_θ is the thermal grashof number, Ec is Eckert number, Pe is Peclet number, $\frac{dp}{\partial z}$ is pressure gradient.

$\mathrm{Re}=\frac{U_{s1}r_2}{v_0}$ is the Reynolds number, $\frac{Ec}{\mathrm{Re}}=\frac{\mu_0U_{s1}^2}{\rho_0c_pU_{s1}(T_{s1}-T_0)r_2}$, $Pe=\frac{\rho_0c_pU_{s1}r_2}{k}$

3.2 Solution via Polynomial Approximation Method (PAM)

Here, we let

$$\frac{dp}{\partial z}=\lambda\, e^{-mt} \tag{15}$$

and $0<c<<1$ *and* $Gr_\theta=\beta c$ such that

$$\phi(\eta,t)=\phi_o(\eta,t)+c\,\phi_1(\eta,t)+\ldots \tag{16}$$

$$\theta(\eta, t) = \theta_o(\eta, t) + c\theta_1(\eta, t) + \cdots \quad (17)$$

Then, we assume polynomial solution of the form (see, [10]):

$$\phi_0(r,t) = a_0(t) + a_1(t)\eta + a_2(t)\eta^2 \quad (18)$$

$$\theta_0(r,t) = a_3(t) + a_4(t)\eta + a_5(t)\eta^2 \quad (19)$$

$$\phi_1(r,t) = a_6(t) + a_7(t)\eta + a_8(t)\eta^2 \quad (20)$$

$$\theta_1(r,t) = a_9(t) + a_{10}(t)\eta + a_{11}(t)\eta^2 \quad (21)$$

And we obtain the solution of equations (12) and (13) as:

$$\phi(\eta,t) = ((b_{15} - b_{13}e^{-b_{12}t} + b_{14}e^{-mt}) + (b_{16}e^{-b_{12}t} - b_{17}e^{-mt} - b_{18})\eta - (b_{19}e^{-b_{12}t} - b_{20}e^{-mt} - b_{21})\eta^2) + c(-b_{46}\left(b_{55} + b_{56}\,e^{-b_{50}t} + b_{57}\,e^{-b_{38}t} + b_{58}e^{-2b_{12}t} + b_{59}e^{-(b_{12}+m)t} + b_{60}\,e^{-b_{12}t} + b_{61}\,e^{-2mt} + b_{62}e^{-mt} + b_{63}\,e^{-(b_{12}+b_{38})t} - b_{64}e^{-(m+b_{38})t} - b_{65}]e^{-3b_{12}t} + b_{66}e^{-(m+2b_{12})t} + b_{67}e^{-(b_{38}+2m)t} + b_{68}e^{-3mt}\right) + b_{47}\left(b_{55} + b_{56}\,e^{-b_{50}t} + b_{57}\,e^{-b_{38}t} + b_{58}e^{-2b_{12}t} + b_{59}e^{-(b_{12}+m)t} + b_{60}\,e^{-b_{12}t} + b_{61}\,e^{-2mt} + b_{62}e^{-mt} + b_{63}\,e^{-(b_{12}+b_{38})t} - b_{64}e^{-(m+b_{38})t} - b_{65}]e^{-3b_{12}t} + b_{66}e^{-(m+2b_{12})t} + b_{67}e^{-(b_{38}+2m)t} + b_{68}e^{-3mt}\right)\eta. - b_{48}\left(b_{55} + b_{56}\,b_{57}\,e^{-b_{38}t} + b_{58}e^{-2b_{12}t} + b_{59}e^{-(b_{12}+m)t} + b_{60}\,e^{-b_{12}t} + b_{61}\,e^{-2mt} + b_{62}e^{-mt} + b_{63}\,e^{-(b_{12}+b_{38})t} - b_{64}e^{-(m+b_{38})t} - b_{65}]e^{-3b_{12}t} + b_{66}e^{-(m+2b_{12})t} + b_{67}e^{-(b_{38}+2m)t} + b_{68}e^{-3mt}\right)\eta^2\ ) \quad (22)$$

$$\theta(\eta,t) = \left(b_{22} - b_{23}(-b_{39} + b_{40}\,e^{-b_{38}t} - b_{41}e^{-2b_{12}t} - b_{42}e^{-(b_{12}+m)t} - b_{43}e^{-b_{12}t} - b_{44}e^{-2mt} - b_{45}e^{-2mt})\right) + \left(b_{24}(-b_{39} + b_{40}\,e^{-b_{38}t} - b_{41}e^{-2b_{12}t} - b_{42}e^{-(b_{12}+m)t} - b_{43}e^{-b_{12}t} - b_{44}e^{-2mt} - b_{45}e^{-2mt}) - b_{27}\right)\eta - \left(b_{26}(-b_{39} + b_{40}\,e^{-b_{38}t} - b_{41}e^{-2b_{12}t} - b_{42}e^{-(b_{12}+m)t} - b_{43}e^{-b_{12}t} - b_{44}e^{-2mt} - b_{45}e^{-2mt}) - b_{27}\right) + c(-b_{69}\ (b_{83}e^{-b_{12}t} + b_{84}e^{-(b_{12}+b_{50})t} + b_{85}e^{-(b_{12}+b_{38})t} + b_{86}e^{-3b_{12}t} + b_{87}e^{-(m+2b_{12})t} +$$

$$b_{88}e^{-2b_{12}t} + b_{89}e^{-(b_{12}+2m)t} + b_{90}e^{-(m+b_{12})t} + b_{81}e^{-(2b_{12}+b_{38})t} - b_{92}e^{-(m+b_{12}+b_{38})t} - b_{93}e^{-4b_{12}t} + b_{94}e^{-(m+3b_{12})t} + b_{95}e^{-(2m+2b_{12})t}\ b_{86}e^{-(b_{12}+3m)t} - b_{97}e^{-mt} - b_{98}e^{-(m+b_{50})t} + b_{99}e^{-(m+b_{38})t} - b_{100}e^{-3mt} - b_{101}e^{-2mt} + b_{102}e^{-(2m+b_{38})t} - b_{103}e^{-4mt} + b_{104} - b_{105}e^{-b_{50}t} - b_{106}e^{-b_{38}t} + b_{107}e^{-b_{73}t}) + b_{70}\ (b_{83}e^{-b_{12}t} + b_{84}e^{-(b_{12}+b_{50})t} + b_{85}e^{-(b_{12}+b_{38})t} + b_{86}e^{-3b_{12}t} + b_{87}e^{-(m+2b_{12})t} +$$

$$b_{88}e^{-2b_{12}t} + b_{89}e^{-(b_{12}+2m)t} + b_{90}e^{-(m+b_{12})t} + b_{81}e^{-(2b_{12}+b_{38})t} - b_{92}e^{-(m+b_{12}+b_{38})t} - b_{93}e^{-4b_{12}t} + b_{94}e^{-(m+3b_{12})t} + b_{95}e^{-(2m+2b_{12})t}\ b_{86}e^{-(b_{12}+3m)t} - b_{97}e^{-mt} - b_{98}e^{-(m+b_{50})t} + b_{99}e^{-(m+b_{38})t} - b_{100}e^{-3mt} - b_{101}e^{-2mt} + b_{102}e^{-(2m+b_{38})t} - b_{103}e^{-4mt} + b_{104} - b_{105}e^{-b_{50}t} - b_{106}e^{-b_{38}t} + b_{107}e^{-b_{73}t})\eta - b_{71}\ (b_{83}e^{-b_{12}t} + b_{84}e^{-(b_{12}+b_{50})t} + b_{85}e^{-(b_{12}+b_{38})t} + b_{86}e^{-3b_{12}t} + b_{87}e^{-(m+2b_{12})t} +$$

$b_{88}e^{-2b_{12}t} + b_{89}e^{-(b_{12}+2m)t} + b_{90}e^{-(m+b_{12})t} + b_{81}e^{-(2b_{12}+b_{38})t} - b_{92}e^{-(m+b_{12}+b_{38})t} - b_{93}e^{-4b_{12}t} + b_{94}e^{-(m+3b_{12})t} + b_{95}e^{-(2m+2b_{12})t}\ b_{86}e^{-(b_{12}+3m)t} - b_{97}e^{-mt} - b_{98}e^{-(m+b_{50})t} + b_{99}e^{-(m+b_{38})t} - b_{100}e^{-3mt} - b_{101}e^{-2mt} + b_{102}e^{-(2m+b_{38})t} - b_{103}e^{-4mt} + b_{104} - b_{105}e^{-b_{50}t} - b_{106}e^{-b_{38}t} + b_{107}e^{-b_{73}t})\eta^2)$ (23)

Where

$b_i,\ i = 1,..,107$ are presented in the Appendix.

4.0 Result and Discussion

4.1 Overview

The analytical solutions derived using the polynomial approximation method were tested to determine the effect of key dimensionless factors on the transient behaviour of velocity and temperature fields in the vertical micro-annulus. The Eckert number (Ec), Peclet number (Pe), Reynolds number (Re), and space- and temperature-dependent internal heat generation coefficients are all taken into account.

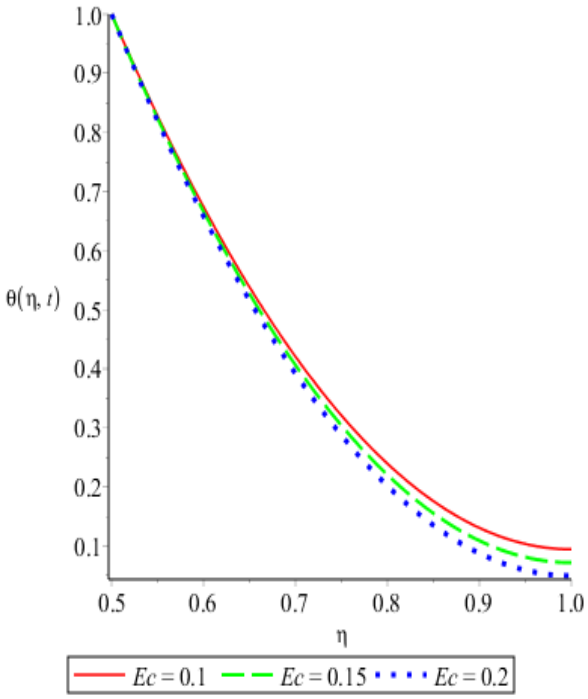

Figure 2: Effect of E_C *in* Fluid Temperature

Figures 2 through 10 show the results. The thermo-fluid behaviour observed in this study is driven by the complicated interaction of buoyant forces, viscous resistance, thermal diffusion, and internal heat generation, all of which are strongly connected via temperature-dependent viscosity.

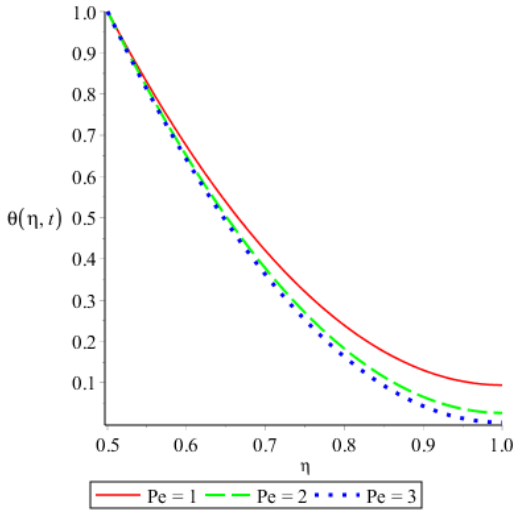

Figure 3: Effect of Peclet (Pe) Number in Fluid Temperature

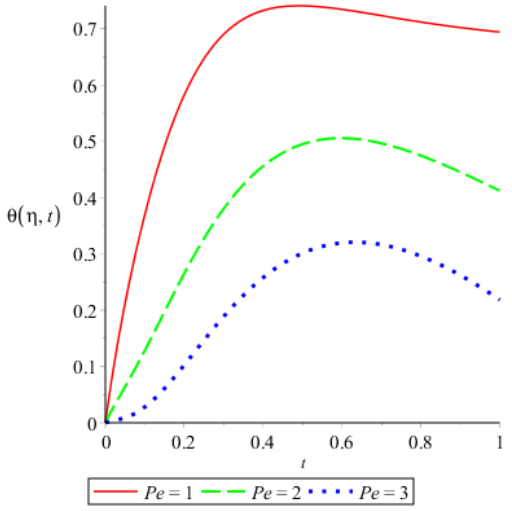

Figure 4: Effect of Peclet (Pe) Number in Fluid Temperature

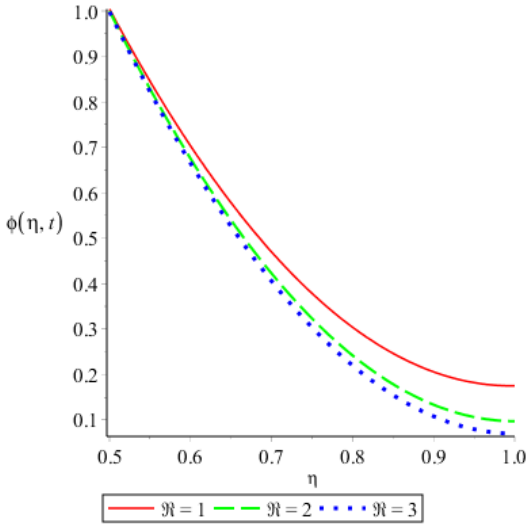

Figure 5: Effect of Reynold Number in Fluid Velocity

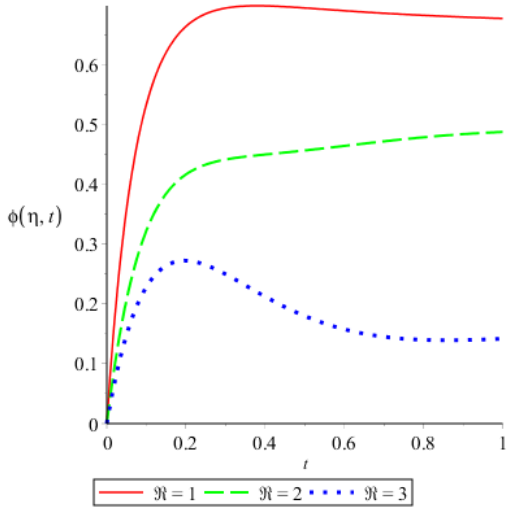

Figure 6: Effect of Reynold Number in Fluid Velocity

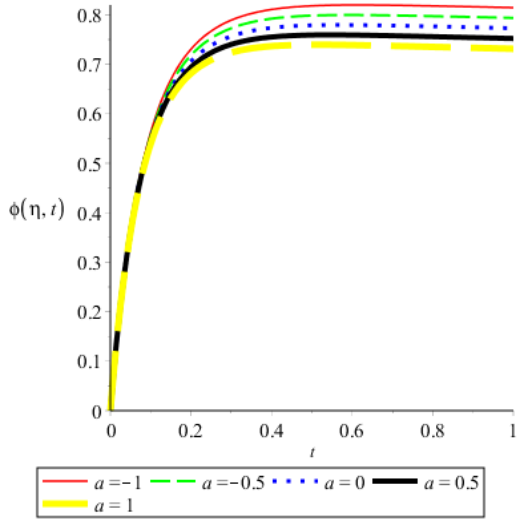

Figure 7: Effect of Heat Generation Parameter in Fluid velocity

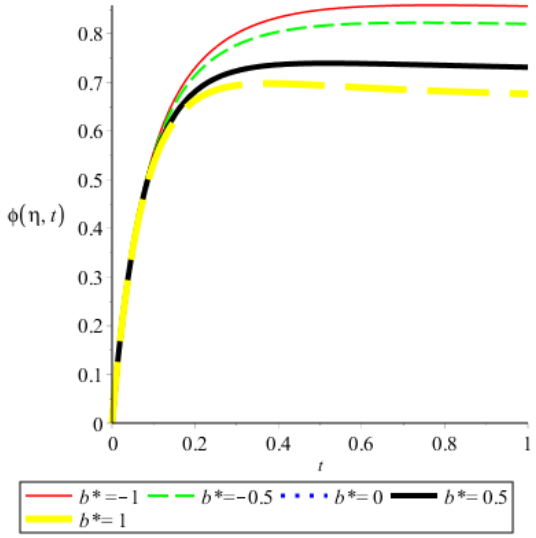

Figure 8: Effect of Heat Generation Parameter in Fluid velocity

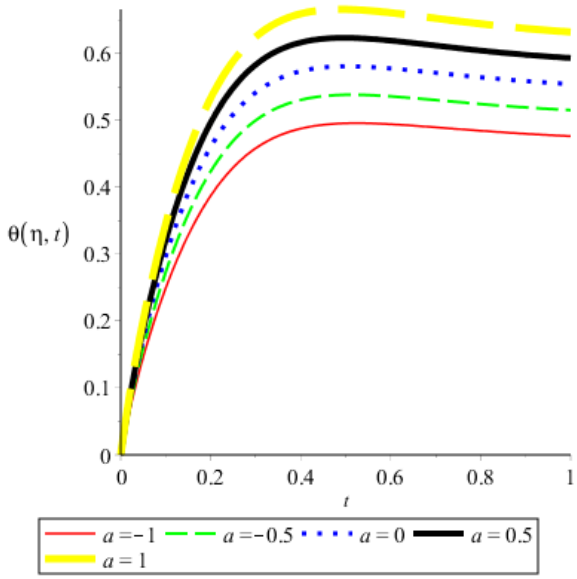

Figure 9: Effect of Heat Generation Parameter in Fluid Temperature

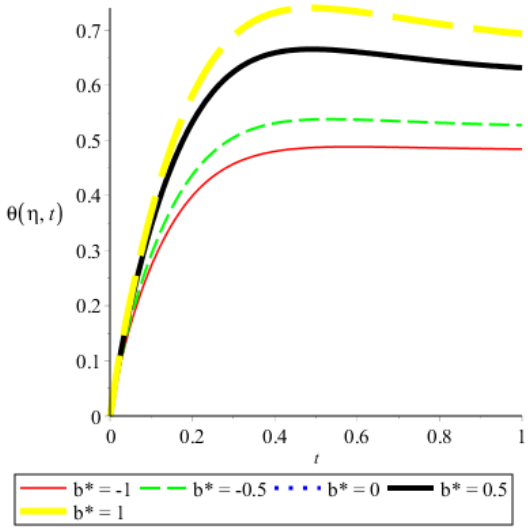

Figure 10: Effect of Heat Generation Parameter in Fluid Temperature

4.2 Effect of the Eckert Number ((E_c)

The Eckert number is the ratio of kinetic energy to enthalpy difference, which quantifies the contribution of viscous dissipation to the fluid's thermal energy. As seen in Figures 2, a rise in Ec reduces fluid temperature in both the spatial and temporal domains. Although viscous dissipation is typically a heat source, its effect in the current structure is mitigated by increased thermal diffusion and convective transport. Higher Ec values increase the conversion of mechanical energy into thermal energy; nevertheless, the ensuing temperature increase amplifies thermal gradients, which improves heat conduction away from the fluid core. This reduces the overall peak temperature. Furthermore, higher viscous effects tend to thicken the velocity boundary layer, slowing fluid motion and restricting convective heat transport. This interaction accounts for the observed temperature reduction with increased Ec.

4.3 The Effect of Peclet Number (Pe)

The Peclet number indicates the relative importance of convective heat transmission vs thermal diffusion. Figures 3 and 4 show that increasing (Pe) causes the fluid temperature to decrease. At larger Pe values, convection takes precedence over diffusion, causing heat to move more quickly along the flow path rather than diffusing across the radial direction. This shortens the residence time of thermal energy inside the fluid domain, resulting in lower temperature levels. This effect is particularly noticeable in micro-scale systems with short characteristic lengths, resulting in sharper temperature gradients and less total heat accumulation.

4.4 The Effect of Reynolds Number (Re)

The Reynolds number represents the ratio of inertial to viscous forces. Figures 5 and 6 indicate that an increase in Re reduces fluid velocity within the annulus. This behaviour may seem paradoxical, but it may be explained by the presence of temperature-dependent viscosity. As the Reynolds number increases, the flow initially accelerates; however, temperature fluctuations alter the viscosity distribution. Viscosity falls in high-temperature zones, changing the velocity profile and increasing flow resistance in cooler regions. The non-uniform viscosity distribution causes an overall dampening of the velocity field. Furthermore, the coupling of buoyancy and forced convection in the vertical structure provides competing flow mechanisms, which further restrict velocity at higher Reynolds numbers.

4.5 Influence of Internal Heat Generation Parameters

(a) Effect of Temperature-Dependent Heat Generation Parameter (Figures 7-8)

Figures 7 and 8 demonstrate the effect of the temperature-dependent heat generation parameter on fluid velocity. It is noticed that increasing this parameter results in a significant reduction in velocity distribution across the flow domain.

This behaviour can be explained by the close link between temperature and momentum fields. As the temperature-dependent heat generation parameter increases, more thermal energy is produced inside the fluid, resulting in a large increase in temperature. Because heat generation is temperature-dependent, the process becomes self-reinforcing: greater temperatures generate more heat, which amplifies the thermal field. The increased temperature gradients create higher buoyant forces within the vertical micro-annulus. These buoyancy effects tend to counter the principal flow direction, resulting in greater flow resistance and reduced fluid velocity. Although increasing temperature may decrease viscosity, this impact is overwhelmed by buoyancy-induced opposition, resulting in an overall reduction of the velocity field.

(b) Effect of Heat Generation Parameter on Temperature (Figures 9 and 10)

Figures 9 and 10 show the effect of the heat generation parameter on fluid temperature distribution. It is clear that increasing the heat generation parameter improves the temperature profile across the flow domain. The apparent temperature increase is caused by the direct input of internal thermal energy to the system. As the heat generation parameter increases, more energy is delivered to the fluid, resulting in higher temperatures and steeper thermal gradients.

This effect is most prominent in microscale systems, where heat accumulates quickly due to limited spatial diffusion.

Furthermore, rising temperature alters fluid properties, particularly viscosity, altering overall thermo-fluid behaviour. As previously noted, the increased temperature field intensifies buoyant forces, which can have an impact on velocity distribution. Overall, the findings show that the heat generation parameter is crucial in influencing the thermal properties of the flow, with higher values resulting in significant temperature increases within the micro-annulus.

4.6 Combined Behaviour of Velocity and Temperature Fields

The data show an inverse link between fluid temperature and velocity. This coupling is caused by the viscosity-temperature relationship. As temperature rises, viscosity normally decreases, affecting momentum diffusion within the fluid. However, in the current arrangement, the dominating process is the increase in buoyant forces owing to temperature increases. These buoyancy effects counter the principal flow direction in some locations, resulting in a drop in velocity despite a decrease in viscosity. This demonstrates the complicated interplay of thermal and hydrodynamic effects in mixed convection systems.

4.7 Transient Characteristics

The transient analysis shows that temperature and velocity fields change nonlinearly over time before reaching steady-state values. The temperature rises quickly at first as thermal energy accumulates within the system. This is followed by a gradual stabilization when heat transmission mechanisms like conduction and convection redistribute energy across the fluid domain.
Similarly, the velocity field undergoes an initial adjustment phase caused by the commencement of flow and the formation of boundary layers. The combination of viscous forces, buoyancy effects, and thermal gradients eventually results in a balanced condition in which the velocity profile stabilizes.

These transient behaviours are especially important in micro-scale systems, where rapid heat response and short time scales are key in deciding performance. The findings underscore the need of taking into consideration time-dependent effects when designing and analyzing such systems.

4.8 Engineering Implications

The results demonstrate that internal heat generation and temperature-dependent viscosity significantly influence flow and heat transfer in micro-annular systems. The ability to control parameters such as Peclet number, Eckert number, and heat generation coefficients provides a means of optimizing thermal performance.

These findings are particularly relevant for:

- micro heat exchangers
- electronic cooling systems
- energy storage devices

- microfluidic reactors

where precise thermal management is essential for efficiency and reliability.

It is worth noting that the effects shown in Figures 2–10 are significant for investigating the influence of heat generation and absorption on flowing fluids.

5.0 Conclusion

This study conducted an analytical analysis of transient mixed convection flow and heat transmission in a vertical micro-annulus, accounting for temperature-dependent viscosity, viscous dissipation, and internal heat generation effects. The governing equations were converted into a dimensionless form and solved using a polynomial approximation method, which allowed important flow and thermal parameters to be evaluated. The findings show that internal heat generation greatly raises fluid temperature while lowering fluid velocity due to increased thermal buoyancy effects and viscosity changes. The Eckert and Peclet numbers were found to reduce temperature distributions, demonstrating that viscous dissipation and thermal diffusion have the greatest influence on energy transport. In contrast, increasing the Reynolds number reduces fluid velocity, indicating the interplay of inertial and viscous forces in the flow domain.

The study also demonstrates a substantial relationship between temperature and velocity fields, which is primarily controlled by viscosity change and energy dissipation mechanisms. These findings emphasize the relevance of considering temperature-dependent fluid characteristics when modelling micro-scale convection processes.

Overall, the analytical solutions reported in this paper provide useful information about the transient behaviour of mixed convection in micro-annular systems. The findings are applicable to the design and optimization of thermal systems such as micro heat exchangers, cooling devices, and energy systems, where precise control of heat transfer and fluid flow is required. Future work should focus on model validation using numerical simulations or experimental data, as well as expanding the analysis to include non-Newtonian fluids and more complex boundary conditions.

References

Abderrahmane, A., Younis, O., Al-Khaleel, M., Laidoudi, H., Akkurt, N., Guedri, K., & Marzouki, R. (2022). Mixed convection heat transfer in thermal energy storage systems. *Nanomaterials*, 12(19), 3270.

Bouchraba, W. (2025). Numerical simulation of mixed convection in concentric annular cylinders with internal heat generation. *Thermal Science*.

Jha, B. K., & Aina, B. (2018). Mixed convection flow in a vertical micro-annulus having temperature-dependent viscosity: An exact solution. *Journal of Nanofluids*, 7, 1–8.

Nabwey, H. A. (2024). Effects of temperature-dependent viscosity and thermal conductivity on convection flow. *Journal of Thermal Analysis and Calorimetry*.

Sheikholeslami, M., Vajravelu, K., & Rashidi, M. M. (2016). Forced convection heat transfer in annular systems under variable magnetic field. *International Journal of Heat and Mass Transfer*, 92, 339–348.

Finlayson, B.A., 1972. *The Method of Weighted Residuals and Variational Principles*. New York: Academic Press.

Jha, B.K. and Aina, B., 2018. Mixed convection flow in a vertical micro-annulus with temperature-dependent viscosity: An exact solution. *Journal of Nanofluids*, 7, pp.1–8.

Sheikholeslami, M., 2020. Numerical investigation of convective heat transfer in complex geometries. *Case Studies in Thermal Engineering*, 21, 100678.

Nabwey, H.A., 2024. Effects of temperature-dependent viscosity and thermal conductivity on convection flow. *Journal of Thermal Analysis and Calorimetry*.

Reddy, J.N., 1993. *An Introduction to the Finite Element Method*. New York: McGraw-Hill.

Bejan, A., 2013. *Convection Heat Transfer*. 4th ed. Hoboken: Wiley.

Bartwal, N., et al. (2025). *Application of meshless methods to mixed convection flow problems*.

Sheikholeslami, M. (2020). Numerical investigation of convective heat transfer in complex geometries. *Case Studies in Thermal Engineering*, 21, 100678.

Vajjha, R. S., & Das, D. K. (2015). Experimental determination of viscosity and thermal conductivity of nanofluids. *International Journal of Heat and Mass Transfer*, 80, 842–851.